SOLAR MULTI-CONJUGATE ADAPTIVE OPTICS AT THE DUNN SOLAR TELESCOPE

T. Rimmele , S. Hegwer, K. Richards, F. Woeger
National Solar Observatory[1]*, Sunspot, NM-88349, USA*
J. Marino
University of Florida, Gainesville, FL
National Solar Observatory, Sunspot, NM-88349, USA
D. Schmidt, T. Waldmann
Kiepenheuer Institute, Freiburg, Germany

1. INTRODUCTION

Solar adaptive optics has become an indispensable tool at ground based solar telescopes. Driven by the quest for ever higher spatial resolution observations of the Sun solar adaptive optics are now operated routinely at major ground based solar telescopes. The current high-resolution solar telescopes, such as the Dunn Solar Telescope (DST), are in the one-meter class and utilize AO for >95 % of the observing time to achieve the diffraction limit at visible and NIR wavelengths. Solar AO [1,2] has revitalized ground-based solar astronomy at existing telescopes. The development of high-order solar AO that is capable of delivering high Strehl in the visible will be absolutely essential for next generation solar telescopes, such as the 4m aperture Advanced Technology Solar Telescope (ATST), which undoubtedly will revolutionize solar astronomy [3].

Solar observations are performed over an extended field of view. The limited size of the isoplanatic patch, over which conventional adaptive optics (AO) provides diffraction limited resolution is a severe limitation. Solar science would benefit greatly from AO correction over large field of views. A single sunspot typically has a size of about 30 arcsec; large active regions often cover a field of 2-3 arcmin. Figure 1 shows an image of solar granulation and embedded magnetic g-band bright points observed near the limb of the sun. The field of view is approximately 120”x 80”. This diffraction limited image was recorded at the Dunn Solar Telescope with high order adaptive optics and post-processed using speckle interferometry. Post-processing is required to achieve the uniform, diffraction limited imaging over such an extended FOV. However, speckle interferometry as well as other post facto restoration methods typically rely on short exposure imaging, which in most cases can not be deployed when quantitative spectroscopy and polarimetry is performed, i.e., long exposures are required. Multi-conjugate adaptive optics (MCAO) is a technique that provides real-time diffraction limited imaging over an extended FOV [4]. The development of MCAO for existing solar telescopes and, in particular, for the next generation large aperture solar telescopes is thus a top priority. The Sun is an ideal object for the development of MCAO since solar structure provides “multiple guide stars” in any desired configuration. It is therefore not surprising that the first successful on-the-sky MCAO experiments were performed at the Dunn Solar Telescope and at a solar telescope on the Canary Islands. However, further development is needed before operational solar MCAO can be implemented at future large aperture solar telescopes such as the ATST on Haleakala[5]. MCAO development must progress beyond these initial proof-of-concept experiments and should include laboratory experiments and on-sky demonstrations under controlled or well characterized conditions as well as quantitative performance analysis and comparison to model predictions.

At the DST we recently implemented a dedicated MCAO bench with the goal of developing well-characterized, operational MCAO. The MCAO system uses 2 deformable mirrors conjugated to the telescope entrance pupil and a layer in the upper atmosphere, respectively. DM2 can be placed at conjugates ranging from 2 km to 10 km altitude. For our initial experiments we have used a staged approach in which the 97 actuator, 76 subaperture correlating Shack-Hartmann solar adaptive optics system normally operated at the DST is followed by the second DM and the tomographic wavefront sensor, which uses three “solar guide stars”. We use modal reconstruction algorithms for both DMs. We have successfully and stably locked the MCAO system on artificial objects (slides), for which

[1] The National Solar Observatory is operated by the Association of Universities for Research in Astronomy under a cooperative agreement with the National Science Foundation, for the benefit of the astronomical community

turbulence screens are generated directly in front of the DMs, as well as solar structure. We varied the height of the upper conjugate between 2 km and 7 km. We recorded strictly simultaneous images after the pupil DM and after the upper layer DM. Comparing these images allows us to evaluate the performance of the MCAO stage and directly compare to the conventional AO. In addition we recorded wavefront sensor telemetry data for closed and open loop. We present preliminary results and discuss future plans.

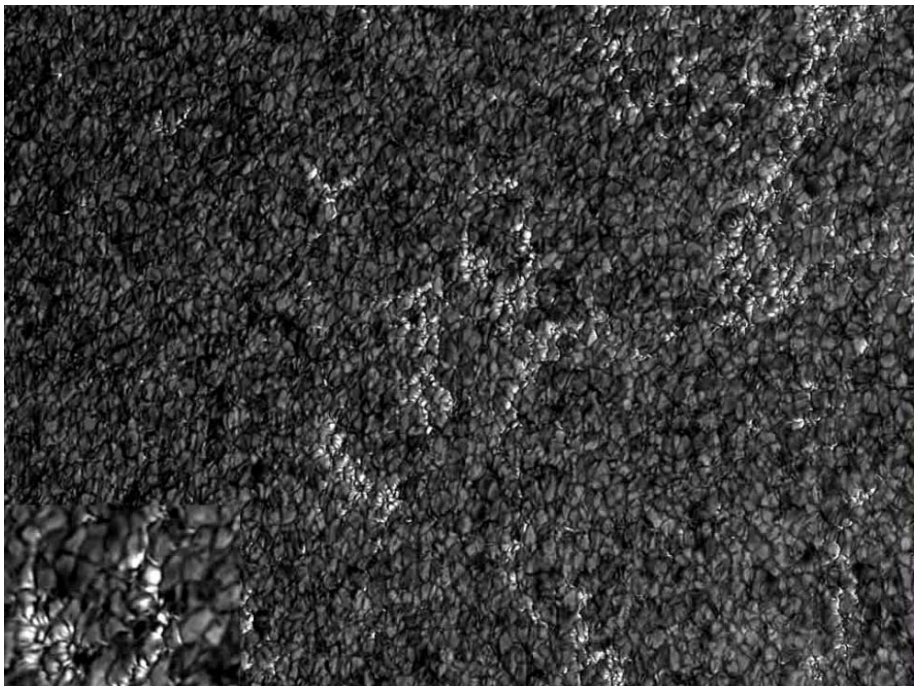

Figure 1: Image of solar granulation and embedded g-band bright points observed near the limb of the sun. The bright points (see zoomed in insert in the lower left corner) are caused by strong magnetic field concentrations. The field of view is approximately 120”x 80”. This diffraction limited image was recorded at the Dunn Solar Telescope with high order adaptive optics and post-processed using speckle interferometry, which yields the uniform, diffraction limited imaging over such an extended FOV.

2. PREVIOUS MCAO EXPERIMENTS AND LIMITATIONS

The initial solar MCAO work performed at NSO [6,7] and at the Kiepenheuer Institute [8] provided proof-of-concept with on-sky experiments at the DST and the German VTT on the Canaries. Both experiments demonstrated the MCAO's ability to extend the corrected FOV. The DST MCAO experiments used two DMs and a MCAO wavefront sensor with three guide regions. Lacking dedicated hardware these experiments utilized existing hardware from the DST conventional AO systems. Due to the constraints given by the existing hardware only three guide regions and a limited number of subapertures (21 per guide region) could be implemented at a reasonable bandwidth. However, since day-time seeing is often dominated by strong ground-layer turbulence a high order correction of the ground-layer is crucial. The 76 subaperture conventional AO system at the 76 cm DST can correct between 60 and 70 KL modes and thus is able to provide good correction for most seeing conditions. By limiting the ground layer correction to only 21 subapertures MCAO work was practically limited to the very best seeing conditions only.

Another severe practical limitation was the fact that in order to set up the MCAO experiment the two operational conventional AO systems had to be disassembled to provide the parts such as DMs and wavefront sensor equipment for the MCAO. Likewise, a complete and time consuming re-assembly and alignment of the conventional AO

systems was necessary after completion of the MCAO experiment. Given the high demand for observing time at the DST this situation was no longer sustainable.

The above mentioned on-sky experiments were performed under unknown atmospheric conditions, i.e., no information about the $Cn^2(h)$ profile above the telescope was available during the experiments. Hence, a detailed comparison of MCAO performance with model predictions was impossible. Furthermore, optimization of parameters such as DM conjugate positions and control algorithms could not be performed. However, before any operational solar MCAO can be designed or built it is crucial to determine how well achieved and expected performance compare and under what conditions and operational parameters.

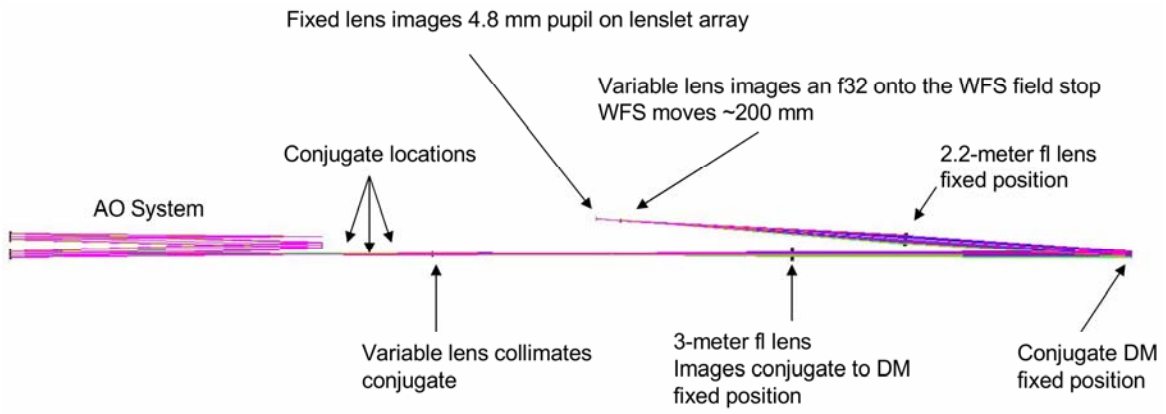

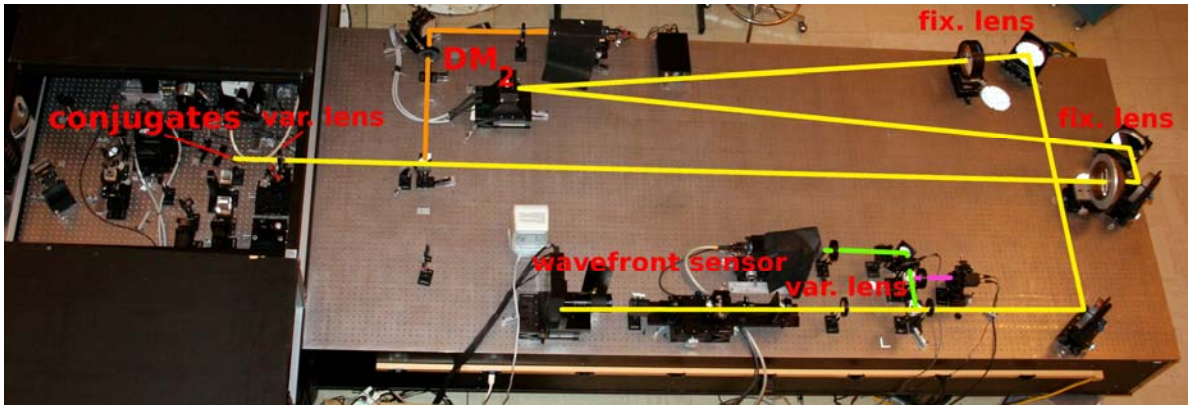

Figure 2. Optical layout of MCAO system at the DST. The first stage consists of the high order DST AO system modified to provide ground-layer AO correction. The second stage uses a three guide-region tomographic WFS. The conjugate height of DM2 can be easily changed between 2-10 km by replacing a collimator lens and moving the WFS while the DM2 remains at a fixed position. The simplicity of this design compared to previous designs has greatly improved the efficiency and progress of the MCAO development work. The picture shows the actual hardware implementation of the MCAO. The beam had to be folded for all components to fit the bench. Scoring cameras are placed behind DM1 and DM2, respectively, in order to obtain strictly simultaneous images of wide field AO and MCAO. The MCAO three guide-region WFS is shown at the lower edge of the image while parts of the high-order, wide-field AO system are visible to the left. Space heaters were used to produce artificial turbulent layers in front of DM1 and DM2 for testing with a pinhole pattern placed in prime focus.

3. MODIFIED MCAO APPROACH AND DESIGN

At the DST we recently implement a dedicated MCAO bench allows for easier and faster and somewhat more permanent implementation of the MCAO experiment. In order to achieve this goal we implemented a staged approach that is uniquely applicable to solar MCAO. Figure 2 shows the optical layout of the MCAO system. The first stage consists of the high order AO system with 76 subapertures and a 97 actuator DM conjugated to ground level. This system is used for normal operations at the DST. The second stage uses a second 97 actuator DM that can be conjugated to an adjustable altitude between 2 and 10 km. The wavefront sensor uses three (3) off-axis guide regions to track granulation or other solar structure. DM2 is on loan from the Big Bear Solar Observatory.

The wavefront sensor of the first stage, high order AO was modified by replacing the lenslet array to provide a wide field of 20”x20” for correlation tracking. The conventional AO uses a small FOV of about 8”x8” and thus provides high order correction more or less on-axis. By computing cross correlations of a large FOV we obtain wavefront aberrations averaged over many field angles and several isoplanatic patch sizes, respectively, effectively providing the desired high order ground layer correction with this first stage of the MCAO system. The principle is demonstrated with Fig. 3, which show the simulated performance a correlating Shack-Hartmann WFS AO system operating on solar granulation. Using an approximate $Cn^2(h)$ profile for the Haleakala site [5] 600 phase screens were generated and the expected performance of the DST AO system was quantified by the Strehl ratio as a function of FOV. The Strehl maps were computed for different WFS FOVs over which the cross-correlation was performed ranging from 4”x4” to 18”x18” using the 20x20 pixels per subfield available in all cases. A more detailed description of the simulation approach and additional results can be found in reference [9]. For small FOV the Strehl is high (S=0.55) at the center field point and decreases rather quickly away from the center. For a FOV of 18”x18” the Strehl is lower and uniform across the entire FOV indicating that a ground layer correction was achieved in this simulation. The task of a MCAO reconstructor is to separate the wavefront correction into the contributions form the ground-layer, which is corrected by DM1, and contributions from the upper layer turbulence, which is corrected by DM2. The simulation of Fig. 3 indicates that the first part can be achieved simply with a wide field correlation tracking WFS, which in this case functions as a ground-layer AO system.

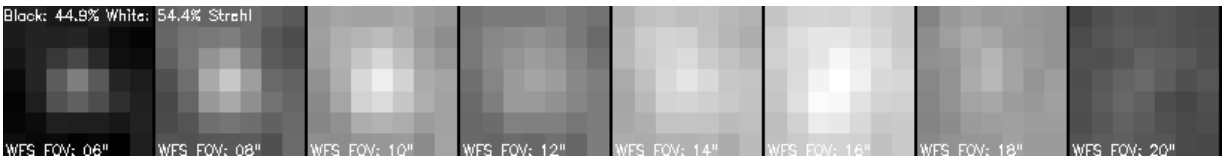

Figure 3. Simulated Strehl maps for different FOVs of the AO76 correlating Shack-Hartmann wavefront sensor. A total of 650 phase maps representing a Haleakala turbulence profile for r0=7cm were averaged. A FOV of 20”x20” results in a reduced but uniform Strehl across the FOV and thus indicates that a ground layer correction is achieved in this way.

The wavefront sensor of the second stage (WFS2) that follows the ground-layer AO utilizes three guide regions of about 10”x10” each. The triangular arrangement of the guide-regions is shown in Fig. 4. The pupil footprints of the guide regions at altitude of 4 km above the telescope are plotted with respect to the metapupil. The spare wavefront sensor camera and processing unit of the high order AO system was used for the second stage of the MCAO experiment. The camera can easily be reprogrammed to accommodate the arrangement of multiple FOVs shown in Fig. 4. The DSP processing unit is used to process 3 guide regions with 21 subapertures each. The system runs at 1.6 kHz frame rate. In principle, any number of subfields can be placed within the large FOV in any desired geometrical arrangement. In practice, the number of guide regions is limited by the processing power of the DSP unit.

Reconstruction matrices that compute actuator commands from the WFS measurements are constructed in the following straight forward way. Karhunen-Loeve (KL) polynomials or alternatively Zernike polynomials are programmed onto the DMs and the corresponding wavefront sensor signals are recorded for each mode. The reconstruction matrices are generated from the resulting interaction matrices by applying a standard Singular Value Decomposition (SVD) algorithm to compute the pseudo inverse. The number of KL modes that can be corrected with DM2 in a stable control loop depends on the seeing conditions and ranges between 15-20 modes. It is likely

that a more sophisticated reconstruction techniques with proper regularization applied would allow us to control additional modes. This will be investigated in experiments that will be performed in the near futures.

Another interesting and unusual feature of this approach is that the control loops for DM1 and DM2 are entirely separated, which results in increased robustness of the MCAO system. Once the loop is closed on the high order ground-layer AO WFS2 measures aberrations caused by the high altitude seeing only.

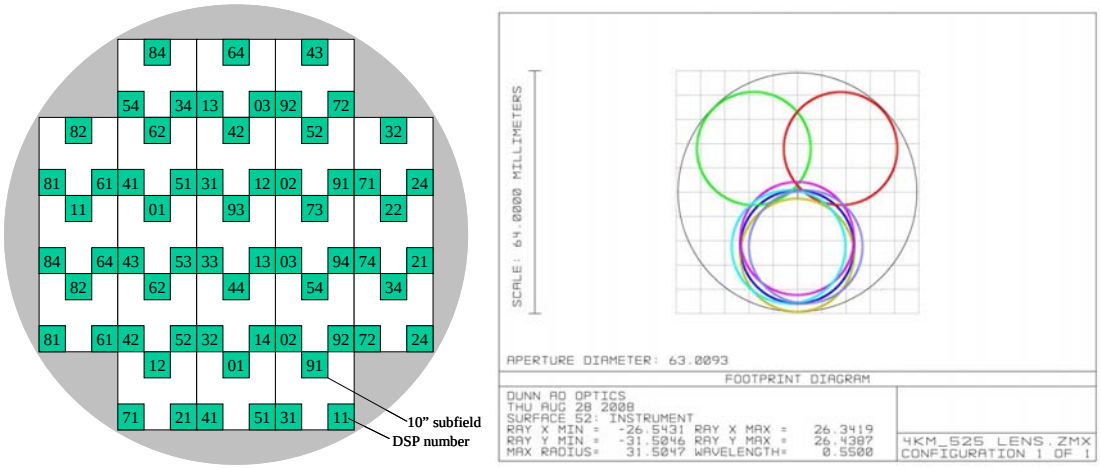

Figure 4: Guide region and WFS geometry (left). The wavefront sensor camera of the MCAO stage reads out three 20x20 pixel (10”x10”) fields arranged in a triangular pattern from within a 52”x52” FOV. The separation between guide regions can be adjusted by simply reprogramming the WFS camera. For the experiment described here the diagonal distance between the centers of the guide regions was about 30 arcsec. The beam footprints of the center field points at an altitude of 4 km are shown as circles within the metapupil on the right. Each of these footprints is sampled with 21 subapertures as shown on the left. The multiple, overlapping circles for one of the fields indicate the coverage caused by the extended field of a guide region.

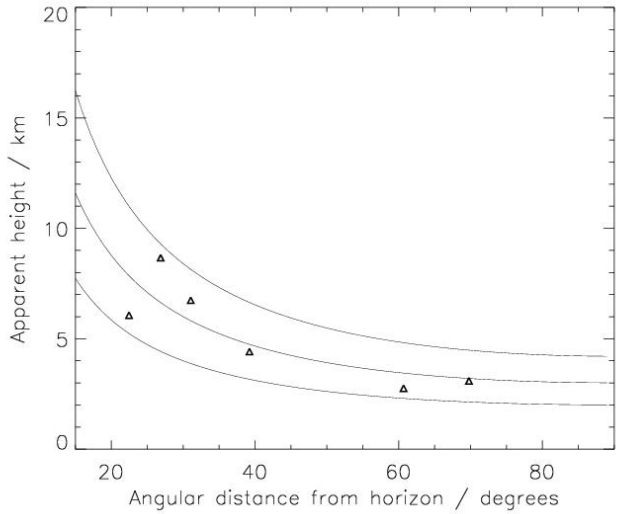

Figure 5: Apparent height of effective turbulence layer above the DST determined from extended FOV wavefront sensing. The triangulation approach is similar to the SLODAR, which used double stars. The solid lines show the apparent height for turbulence layer located at 2, 3 and 4km. The triangles are the actual measurements for Aug. 13, 2008.

4. TURBULENCE PROFILE ESTIMATION

One of the main goals of the DST MCAO experiments is to perform detailed on-sky evaluations and comparison to simulated performance estimations. A crucial ingredient to this effort is knowledge of the turbulence profile above the DST at the time the experiments are performed. A method to determine $Cn^2(h)$ that uses an extended field Shack-Hartmann WFS and is similar to the night-time SLODAR [10] is being developed [11] and will be implemented at the DST. The ultimate goal is to provide close to real-time turbulence profiling. First results are shown in Fig. 5, which plots the apparent height of the dominant turbulence layer above the DST as a function of the angular distance from horizon. These measurements from Aug. 13, 2008 are representative for an observing day at Sac Peak during which seeing conditions are excellent. The real time video images indicated that there was little high altitude (>10 km) turbulence caused by the jet stream dipping far to the south as it is typically present during less favorable seeing conditions. Instead the measurements are consistent with a turbulence layer located between 2 km and 4 km above the telescope. Solar observations are usually performed in the morning hours and ideally the altitude of the conjugate for DM2 should be adjustable on short time scales. This is not practical with the setup shown in Fig. 2. As a compromise we chose a conjugate altitude of 4 km for DM2. Detailed simulations will be used to optimize the location of DM2.

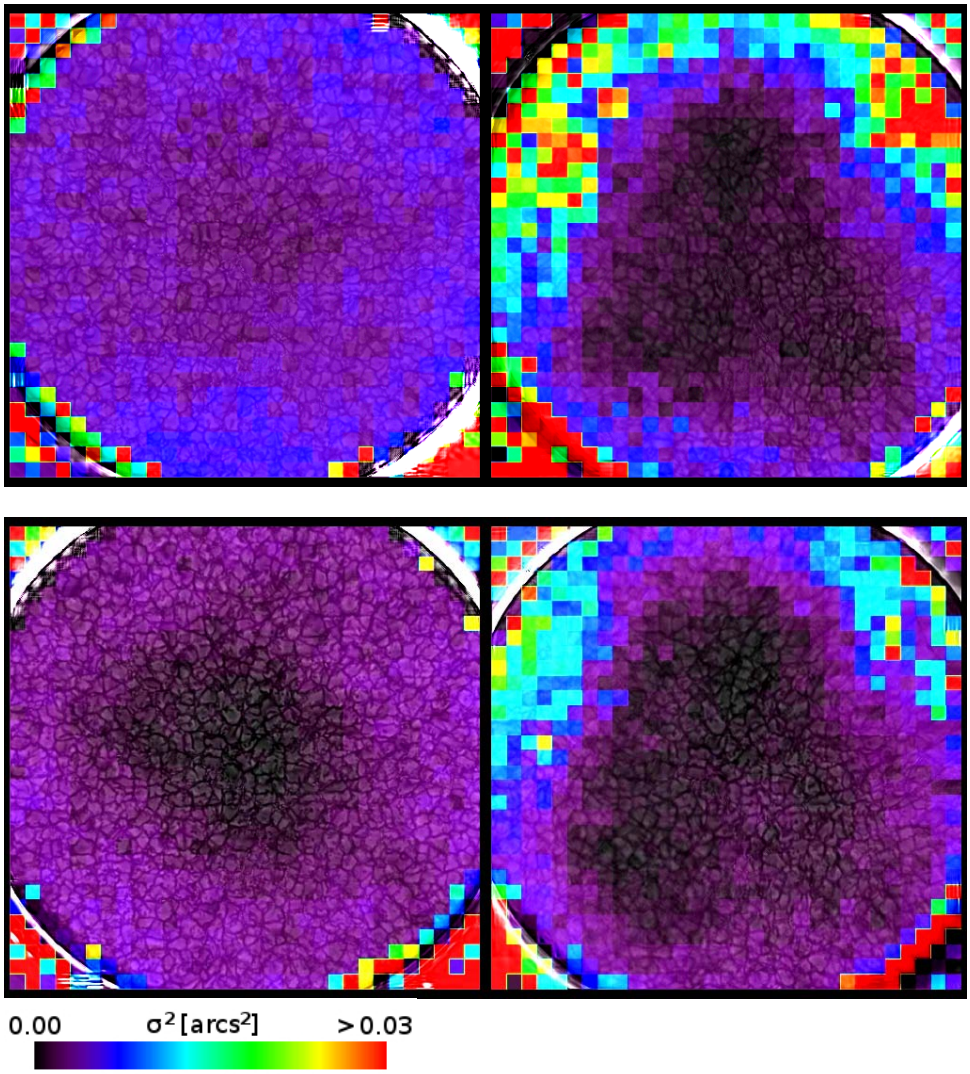

Figure 6: Residual image motion is displayed in a color scale on top of solar granulation. The images on the left were recorded after DM1. Dark areas indicate good correction. The images on the right are recorded after DM2 and demonstrate the ability of the MCAO stage to provide an increased corrected FOV. DM2 corrected 20 KL modes. The FOV is about 60 arcsec

5. RESULTS

The observations were performed during May and Aug. 2008. Bursts of 50 -100 digital 1kx1k images with an exposure time of 10ms were recorded after ground-layer AO correction and after the MCAO correction, respectively. The images were recorded strictly simultaneously at a frame rate of 8 Hz. The observing wavelength was 510 nm (9 nm FWHM) for both channels. During these runs DM2 was positioned at conjugate heights of 2, 4, 5 and 7 km. The best results were achieved with the DM2 at 4 and 5 km conjugates, which is not surprising given the result of Fig. 5, which was obtained during the Aug. 2008 period. The number of modes controlled modes was varied between 9 and 20 KL modes. The control loop quickly became unstable during attempts to control more modes.

The image bursts were processed in two ways. A local correlation algorithm was applied to obtain residual image motion within the extended FOV of about 60" diameter. Residual image motion is easily computed from granulation images and is an indicator for the degree of correction obtained. Alternatively, a speckle reconstruction algorithm [12] was applied, which also outputs residual image motion. The results of both methods are nearly identical. The speckle reconstruction method can provide additional information about residual higher order aberrations. This more detailed analysis is still ongoing and will be reported on at a later time.

Figure 6 shows two examples of residual image motion maps. The granulation image in the background is the speckle reconstruction of the corresponding burst of images. Dark areas in these images indicate good correction. The images on the right are recorded after DM2 and demonstrate the ability of the MCAO stage to provide an increased corrected FOV compared to the conventional AO. DM2 corrected 20 KL modes for these cases. The residual image motion maps recorded after DM1 (left) are not uniform across the FOV indicating that our wide field wavefront sensor approach did not deliver a perfect ground-layer correction but still corrected more efficiently on-axis. This is very apparent for the example shown at the bottom of Fig. 6 and to a lesser degree for the example at the top of the same figure. It appears that for the example shown at the top a ground-layer correction was approximated more closely by the wide field wavefront sensor approach.

The MCAO corrects to a level of less than 0".01 rms and within a triangular shaped FOV of about 40" compared to typically less than 10" of the conventional AO. The location of the guide regions is clearly reflected in the residual image motion maps since the correction is a maximum at these locations. Image motion is actually increased by the MCAO stage in the corners of the FOV where the 3 guide-region wavefront sensor does not provide any information. Naturally, this effect is more prominent as the order of correction on DM2 is increased.

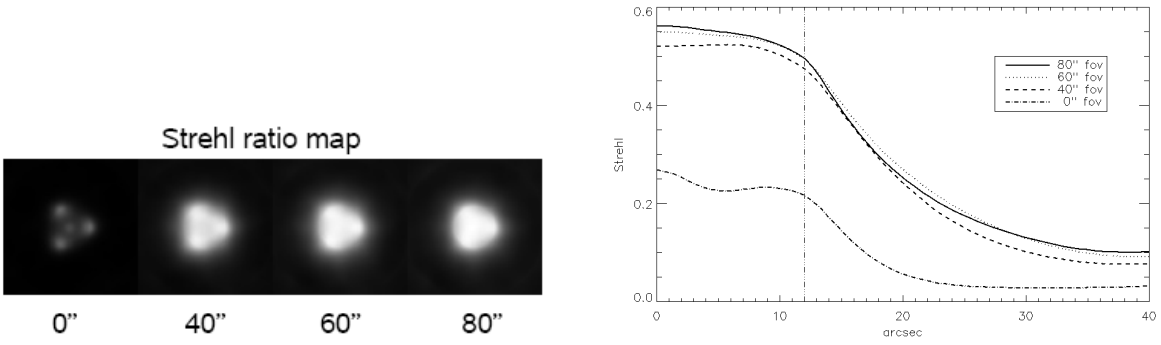

Figure 7. Simulated MCAO performance. Phase screens were produced using a simple two layer atmosphere with a ground-layer at 0 km and a upper layer turbulence at 5km. Strehl maps (left) are computed for different field sizes of the wide field wavefront sensor that drives DM1. The left panel shows Strehl distributions within a 80"x80" FOV for r0=5cm (0km) and r0=20cm(5km). The line plots on the right show an azimuthal average of the Strehl for r0=10cm (0km) and r0=30cm (5km).

6. SIMULATIONS

More insights can be gained by comparing the results of Fig. 6 to simulations of our somewhat unusual two-staged MCAO approach. A series of 300 turbulent phase screens were computed for a simple two layer atmosphere consisting of a ground layer (0 km) with an r0 of 5 cm and one upper layer at 5 km and with an r0 of 20 cm. This turbulence distribution can be considered a very crude approximation of the turbulence profile above the DST during the Aug. 2008 campaign and is only intended to provide a qualitative view of the expected performance. The simulation implements the appropriate wavefront sensors of the two staged approach as well as the two independent control loops. Figure 7 shows the Strehl across a 80"x80" FOV. The free parameter is the FOV of the wide field sensor of the first stage, which varies between a pure on-axis correction to a correlation FOV of 80"x80". Only for large FOVs of 40"x40" or larger can a relatively smooth and even Strehl distribution be achieved, i.e., compared to Fig. 3 a rather large FOV is needed to obtain the desired ground-layer correction with DM1. This is not surprising since the turbulence is assumed to be located low in the atmosphere. Comparison of Figs. 6 and 7 shows qualitative agreement between simulations and observations in the sense that the three guide regions are prominently seen in the Strehl distributions. The Strehl reaches a maximum at the location of the guide regions in both simulations and observations. The dips of the Strehl in between guide regions are more pronounced for small FOVs of the "ground-layer" AO system, i.e., are directly related to the extend to which a true ground-layer correction was achieved with the first stage of our MCAO. We note that the MCAO correction is more uniform and better overall for the example shown at the top of Fig. 6. The left panel of this figure indicates that in this case the first stage of our MCAO effectively operated as ground-layer AO.

7. CONCLUSIONS AND FUTURE WORK

We presented results from our solar MCAO experiment performed at the DST. Our approach, which combines a wide field correlating Shack Hartmann AO system with a three guide-region MCAO stage is somewhat unusual and uniquely applicable to solar MCAO and possibly other extended object AO systems. At the DST this approach allows us to quickly switch from normal operations with conventional AO to the experimental MCAO development work and, in addition, provides without any new hardware required the high order correction of the strong ground-layer, which is dominant during day-typical time seeing. We demonstrated that this approach provides a corrected FOV 3-4 times that of the conventional AO. The strong dependence of the MCAO performance on the FOV of the ground-layer AO wavefront sensor, the size of which is driven by the turbulence distribution, is a concern as are practical concerns such as the number of pixels required to implement an effective ground-layer AO in this way. Future efforts will compare the performance of the two-staged approach with that of a MCAO approach that uses a generalized interaction matrix approach and a global control loop. Simulations indicate that slightly better performance can be achieved with such an approach depending on turbulence distribution and the specific FOV chosen for the wavefront sensor(s). The goal of the MCAO effort at the DST is to provide an AO corrected field that extends over about 1 arcmin and, most importantly, to develop this technology for large aperture solar telescopes such as the ATST. Next steps will include adding additional guide-regions and increase the number of subapertures per guide region. Unfortunately, this can not be achieved with existing hardware. We anticipate using newer DSP technology for this upgrade [13].

REFERENCES

1. Rimmele, T. R., *"Recent Advances in Solar Adaptive Optics"*, 2004**, SPIE 5490,** 34
2. Rimmele, T.~R.: ``Solar Adaptive Optics: Conventional and Multi-Conjugate", Proc. of the 2005 AMOS Technical Conference (Maui Economic Development Board), pp. 575
3. Rimmele, T.; Keil, S.; Wagner, J., 2006, "The unique scientific capabilities of the Advanced Technology Solar Telescope", 36th COSPAR Scientific Assembly. Held 16 - 23 July 2004, in Beijing, China., p.3186
4. Beckers, J. M 1988, *"Increasing the Size of the Isoplanatic Patch with Multiconjugate Adaptive Optics"*, in: Very Large Telescopes and their Instrumentation, ESO Conference and Workshop Proceedings, Proceedings of a ESO Conference on Very Large Telescopes and their Instrumentation, held in Garching, March 21-24, 1988, Garching: European Southern Observatory (ESO), edited by Marie-Helene Ulrich., p.693
5. Rimmele, T., Richards, K., Roche, J.M., Hegwer, S.L., Hubbard, R.P., Hansen, E.R., Goodrich, B., Upton, R.S. "The wavefront correction system for the Advanced Technology Solar Telescope." Advances in Adaptive Optics II., Edited by Ellerbroek, Brent L.; Bonaccini Calia, Domenico., Proceedings of the SPIE, Volume 6272, pp., 627212 (2006).
6. Langlois, M., Moretto, G., Richards, C., Rimmele, T., Hegwer, S., SPIE **5490**, 59
7. Rimmele, Thomas; Richards, Kit; Roche, Jacqueline; Hegwer, Steve; Tritschler, Alexandra, 2006, "Progress with solar multi-conjugate adaptive optics at NSO", SPIE, 6272, 5
8. Berkefeld, Thomas; Soltau, Dirk; von der Lühe, Oskar, 2003, *"Multi-conjugate Adaptive Optics at the Vacuum Tower Telescope, Tenerife"*,in: Adaptive Optical System Technologies II. Edited by Wizinowich, Peter L.; Bonaccini, Domenico. Proceedings of the SPIE **4839**, pp. 544-553
9. Woeger,F. , Rimmele,T., 2008, Applied Optics, submitted
10. Torsten A. Waldmann, Thomas Berkefeld, and Oskar von der Luehe. Turbulence height profiling using wide field of view Hartmann-Shack wavefront sensors, Proc. of the SPIE, 2008
11. Wilson, R.W., "SLODAR: measuring optical turbulence altitude with a Shack-Hartmann wavefront sensor." Mon. Not. R. Astron. Soc. 337, 2002.
12. Woeger, F. , von der Luehe}, O. , Reardon, K. , "Speckle interferometry with adaptive optics corrected solar data", 2008, A&A, 488, 375
13. Richards, K., Rimmele, T., 2008, "Real-time processing for the ATST AO system", AMOS 2008, These Proceedings